Supporting Information

A Hybrid Electrocatalyst with Coordinatively Unsaturated MOF Shell and Hollow Ni_3S_2/NiS Core for OER Application

Jingjing Wang and Hua Chun Zeng*

Department of Chemical and Biomolecular Engineering, Faculty of Engineering, National University of Singapore, 10 Kent Ridge Crescent, Singapore 119260

* Email: chezhc@nus.edu.sg

Contents

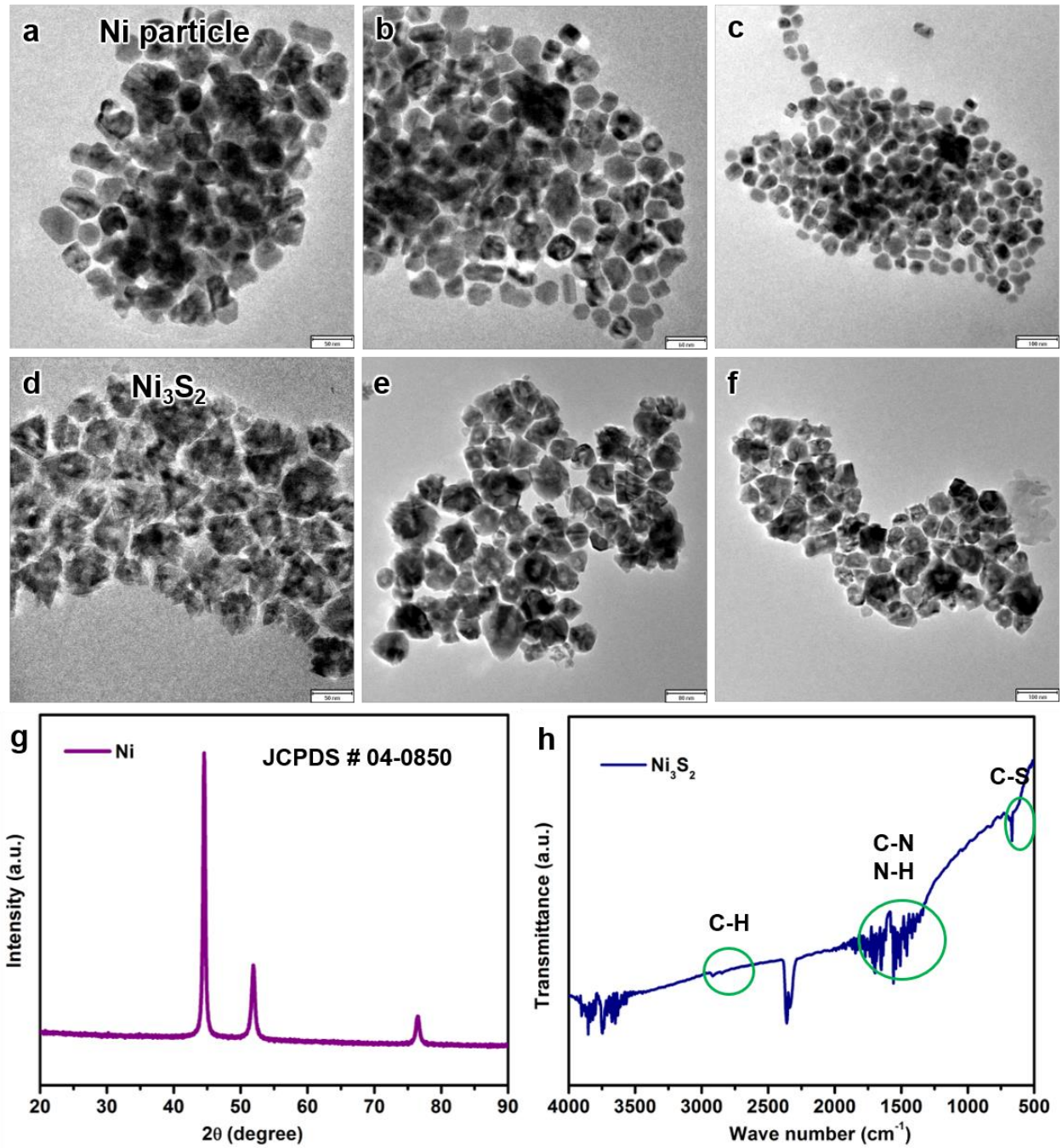

Figure S1. (a-c) TEM images of colloidal Ni nanoparticles, (d-f) TEM images of Ni_3S_2 hollow nanoparticles, (g) XRD pattern of Ni nanoparticles, and (h) FTIR spectrum of organic ligands encapsulated Ni_3S_2 hollow nanoparticles.

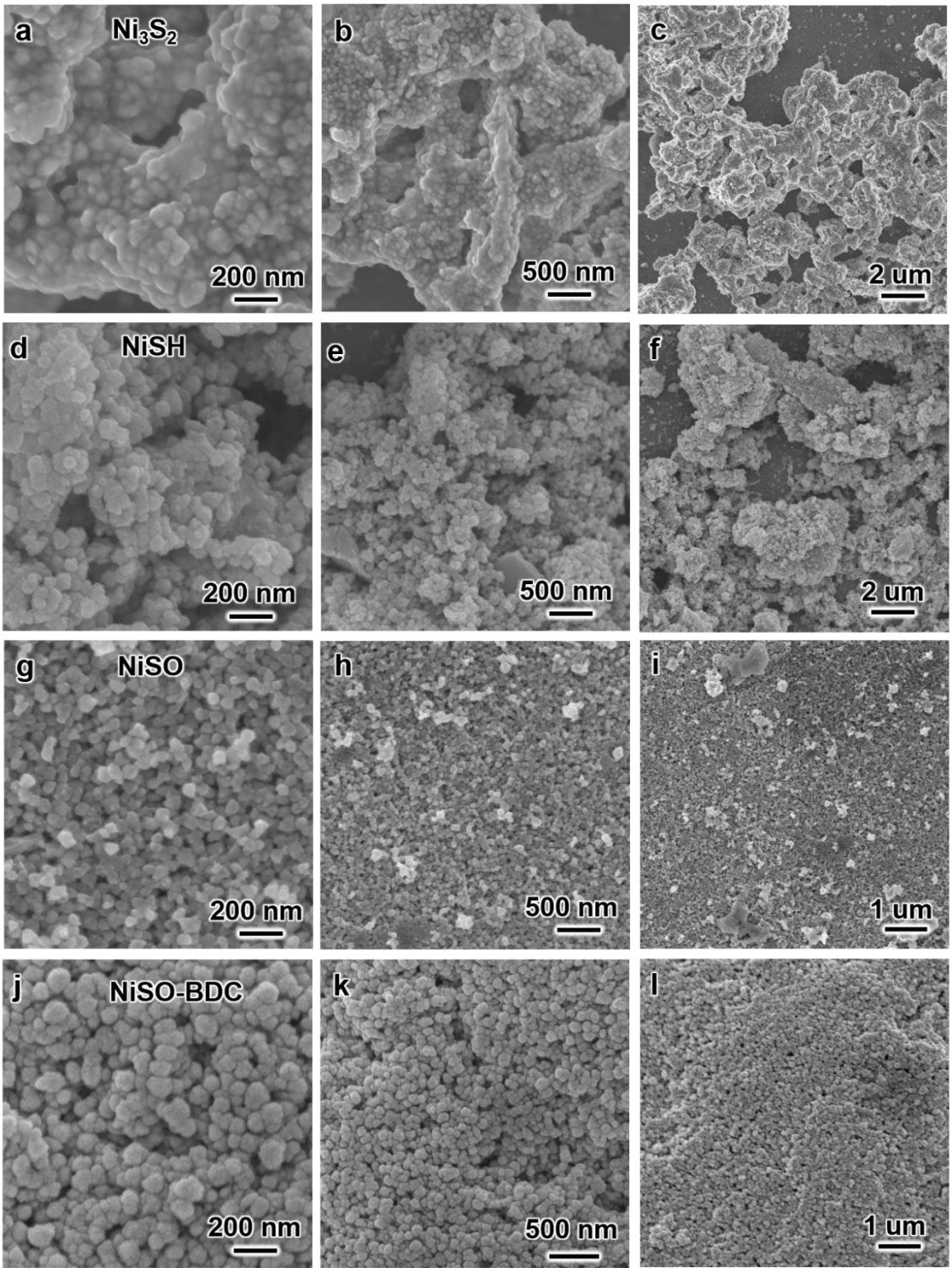

Figure S2. SEM images of (a-c) Ni_3S_2 hollow nanoparticles, (d-f) NiSH hollow nanoparticles (i.e., Ni_3S_2 after heat treatment under 5% H_2/Ar atmosphere), (g-i) NiSO hollow nanoparticles, and (j-l) NiSO-BDC hollow nanoparticles.

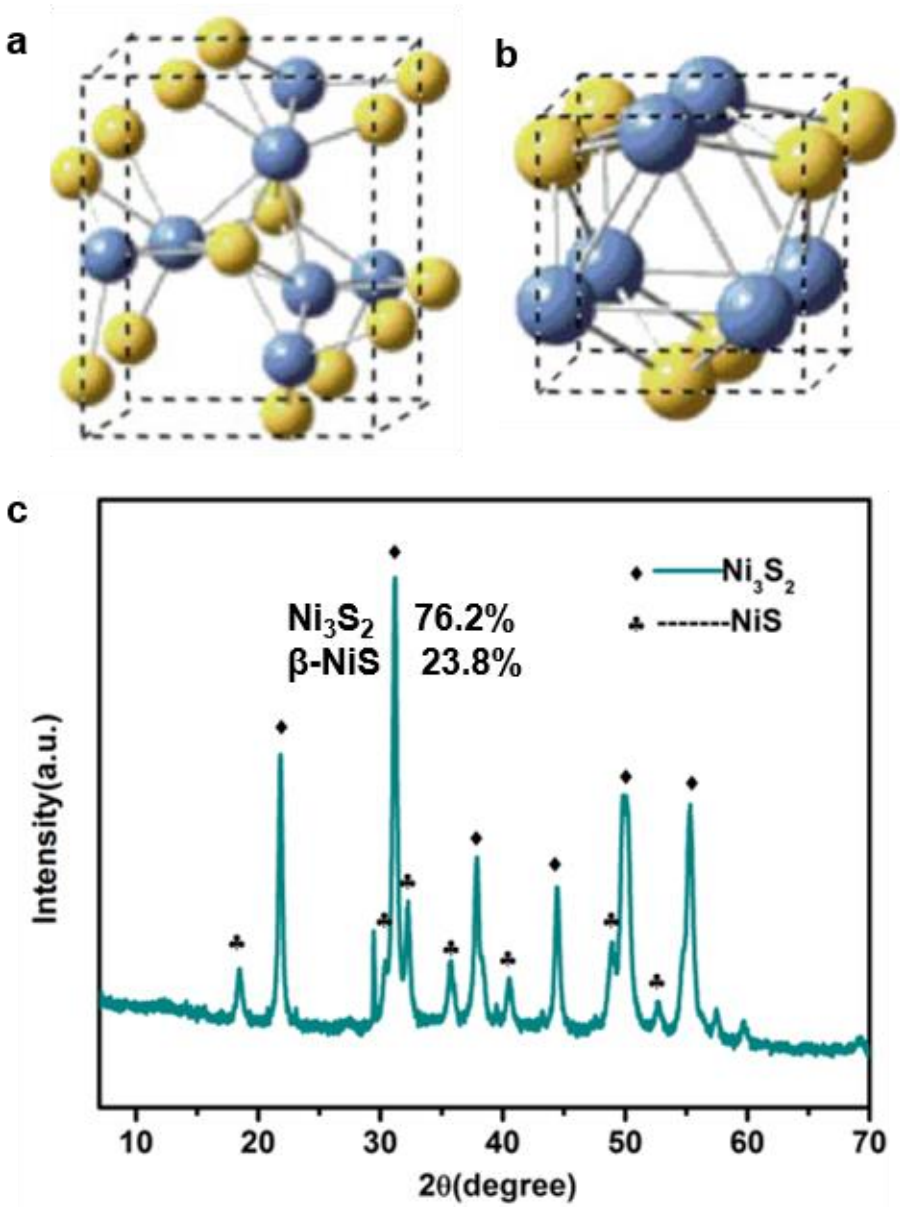

Figure S3. (a, b) Unit cell structures of Ni_3S_2 and NiS respectively,[1] and (c) XRD patterns of NiSO (i.e., Ni_3S_2/NiS) and the calculated weight percentages of Ni_3S_2 and NiS in the NiSO sample.

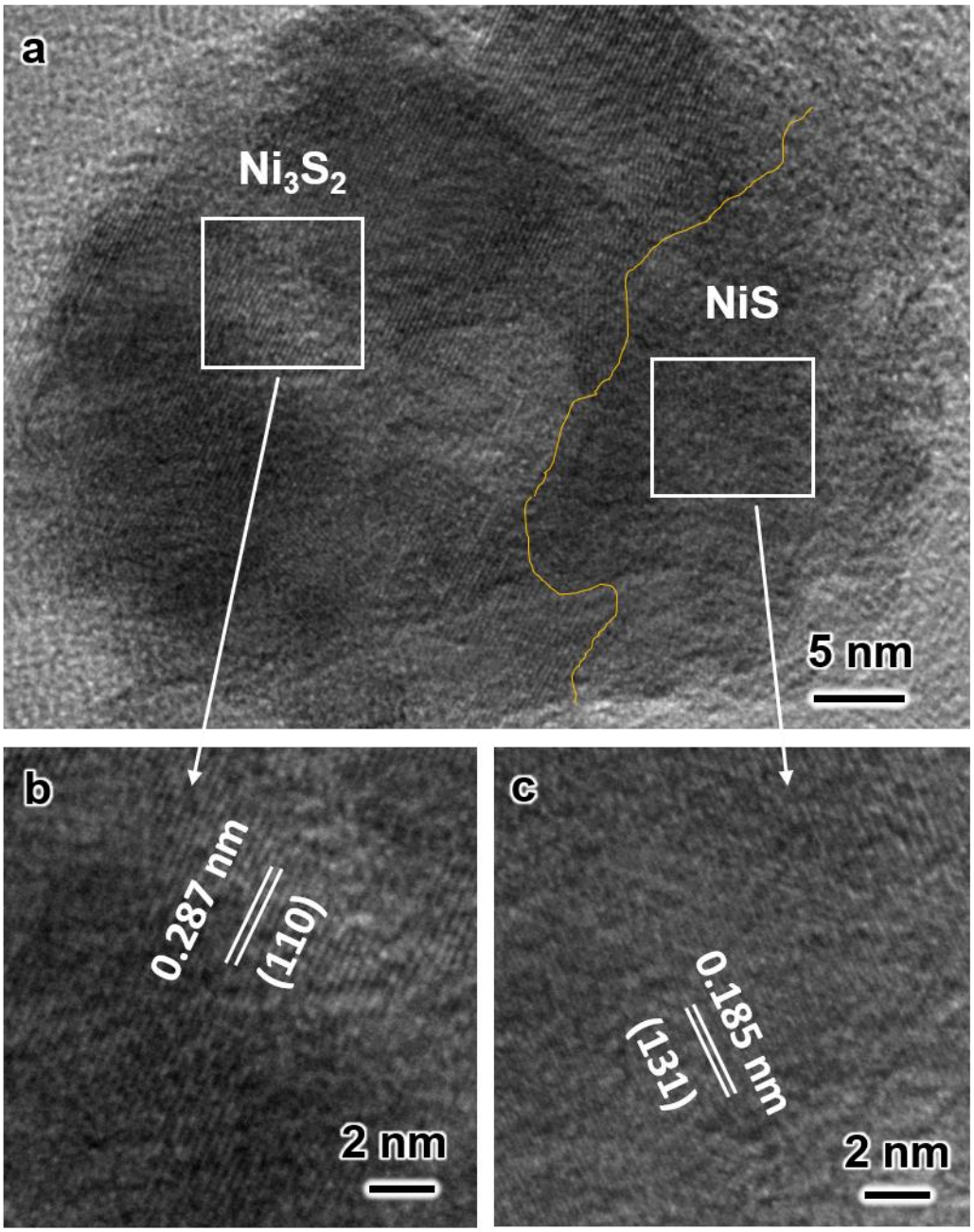

Figure S4. (a) TEM image of a NiSO hollow nanoparticle, and (b and c) high-resolution TEM images for the two framed areas of (a). The yellow thread in (a) indicates the biphasic boundary between Ni_3S_2 and NiS.

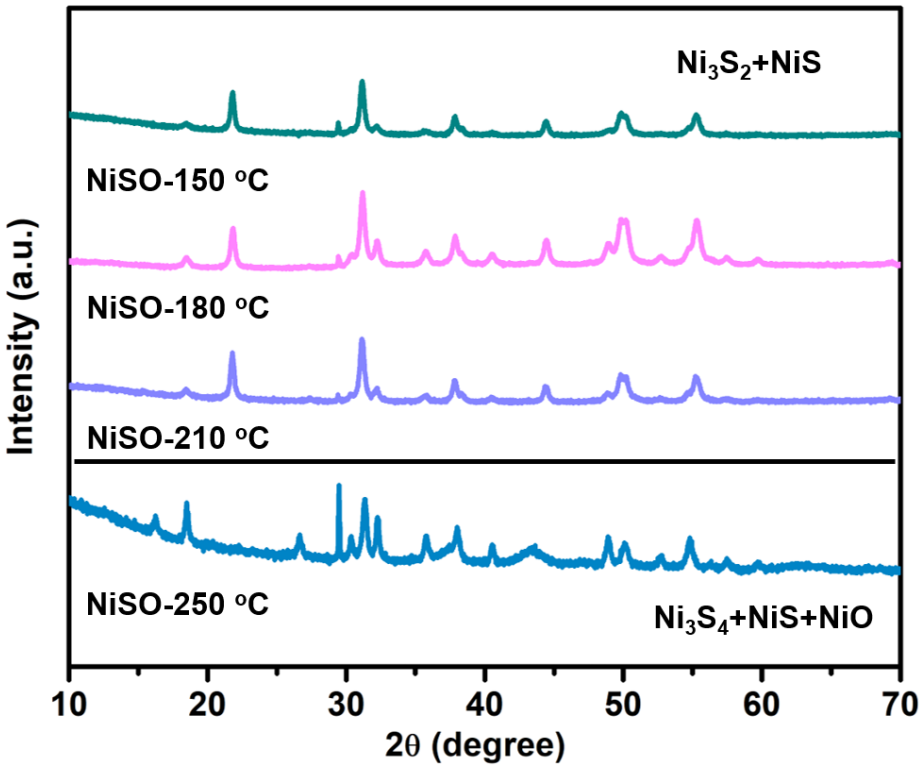

Figure S5. XRD patterns of NiSO (i.e., Ni_3S_2/NiS) treated at different temperatures (150°C, 180 °C, 210 °C, 250 °C) in air environment. See Figure S11 for the peak assignment of NiO phase.

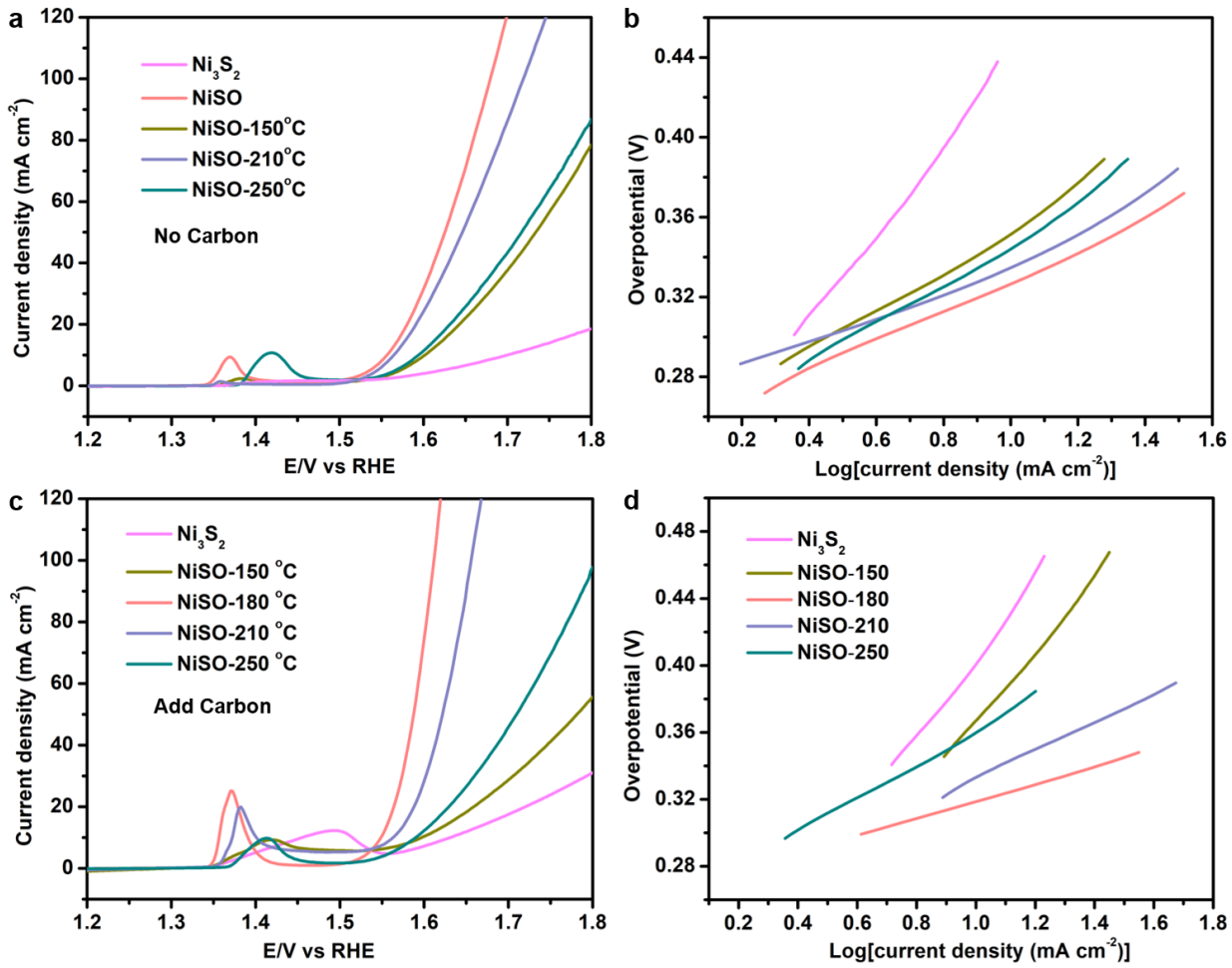

Figure S6. (a) LSVs and (b) the relevant Tafel plots of Ni_3S_2 and NiSO treated at different temperatures tested in 1.0 M KOH without adding carbon. (c) LSVs and (d) the relevant Tafel plots of Ni_3S_2 and NiSO treated at different temperatures tested in 1.0 M KOH with carbon.

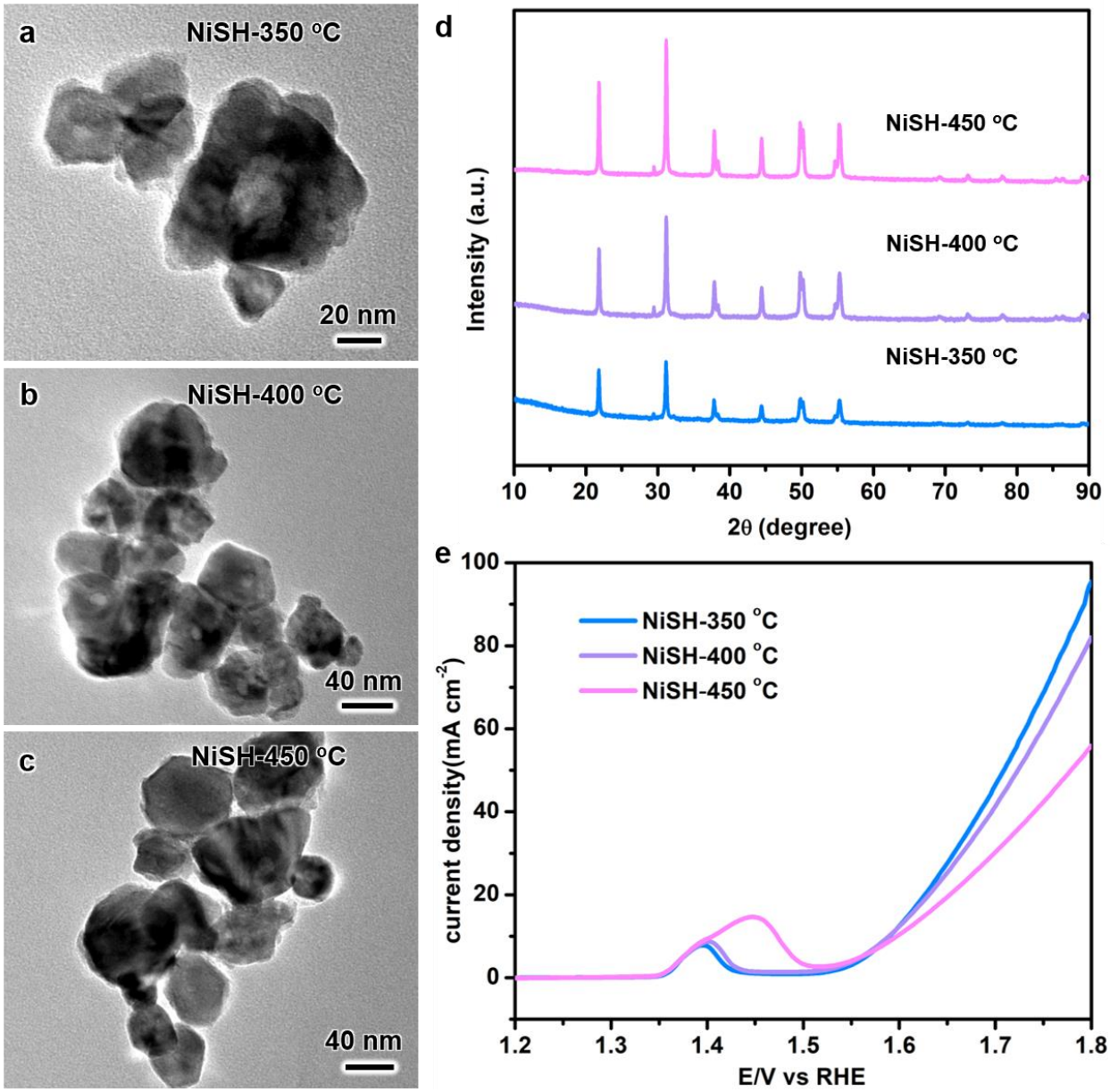

Figure S7. (a-c) TEM images, (d) XRD patterns, and (e) LSVs of NiSH (i.e., Ni_3S_2 after heat treatment under 5% H_2/Ar atmosphere) obtained at 350 °C, 400 °C and 450 °C respectively.

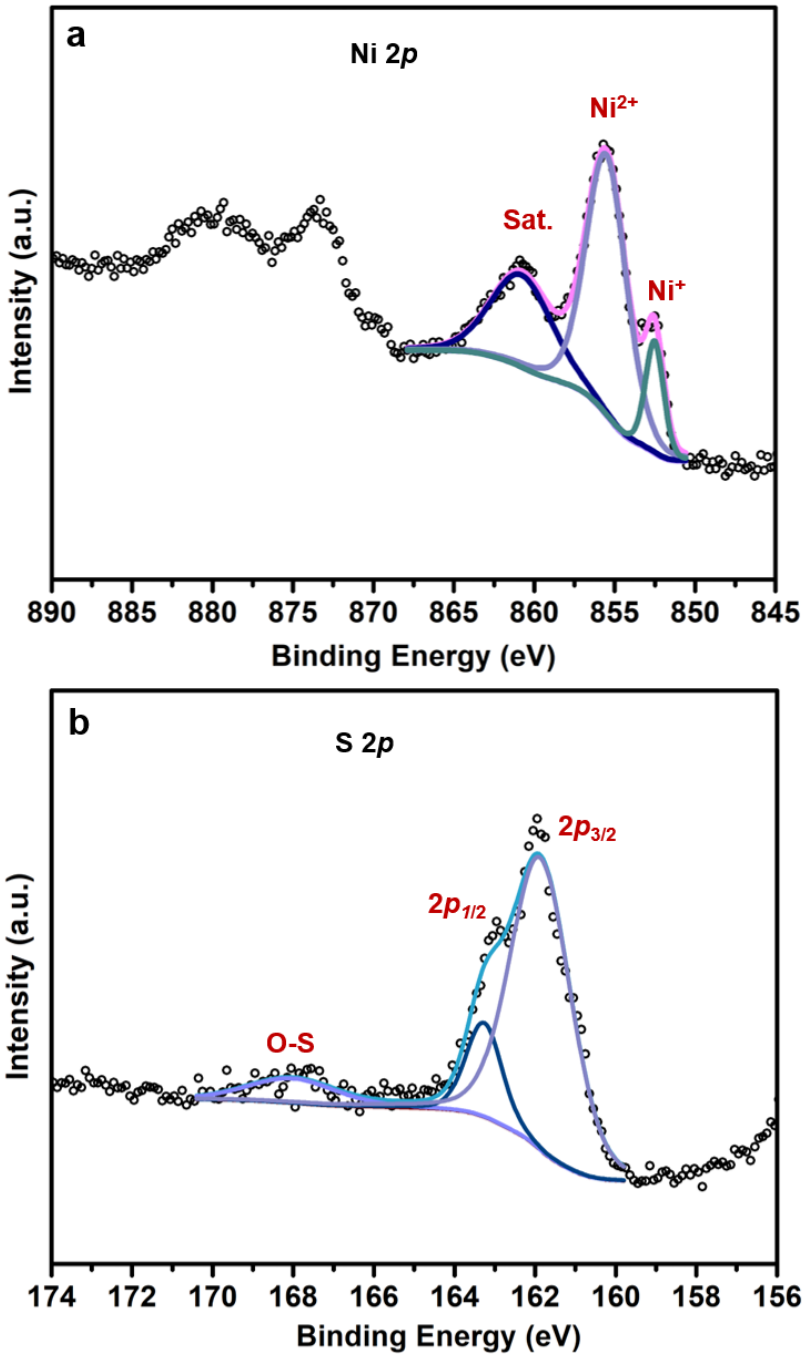

Figure S8. (a) Ni 2*p* and (b) S 2*p* XPS spectra of NiSH-400 ºC.

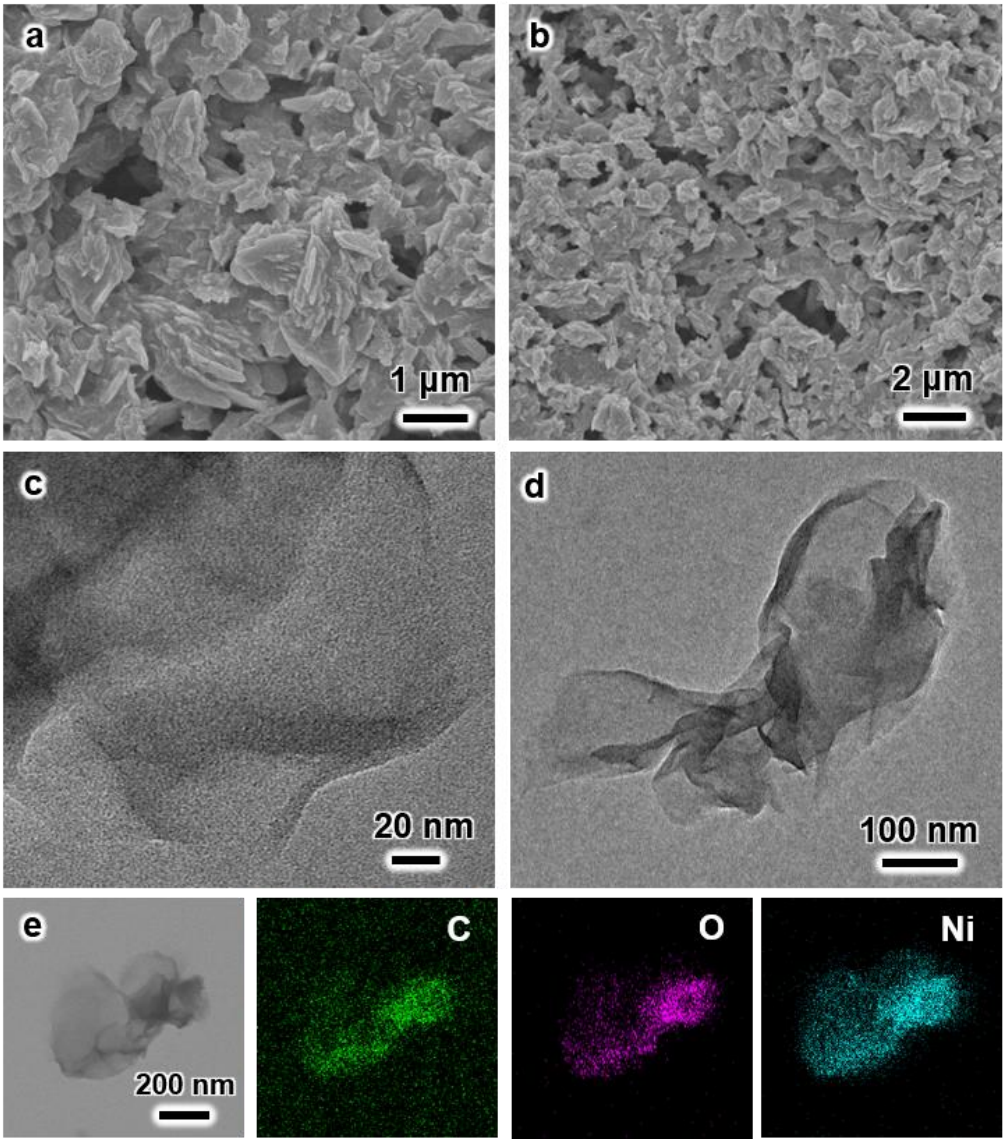

Figure S9. (a, b) SEM images, (c, d) TEM images, and (e) elemental mapping images of the Ni-BDC sample.

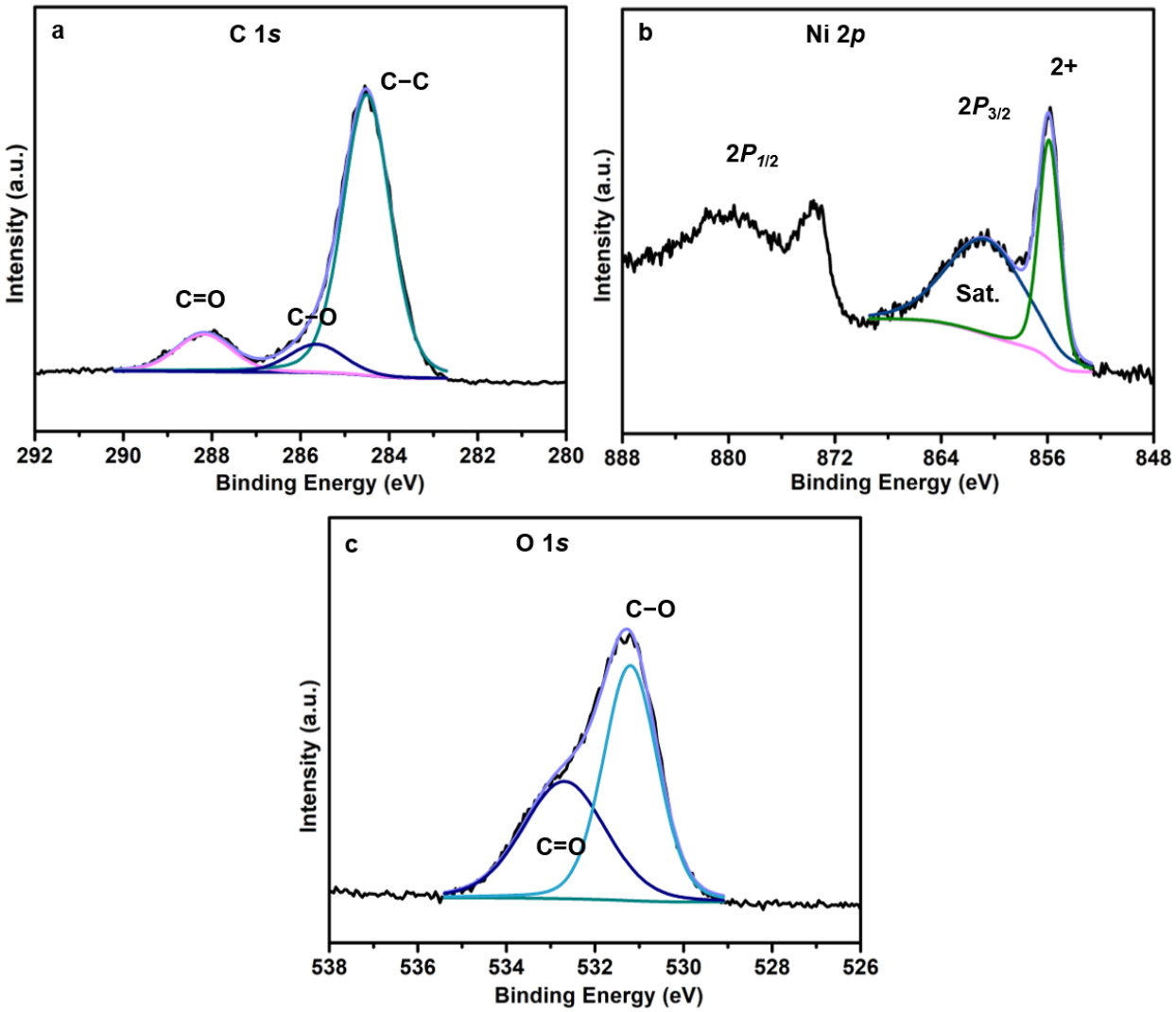

Figure S10. (a) C 1*s*, (b) Ni 2*p*, and (c) O 1*s* spectra of the Ni-BDC sample.

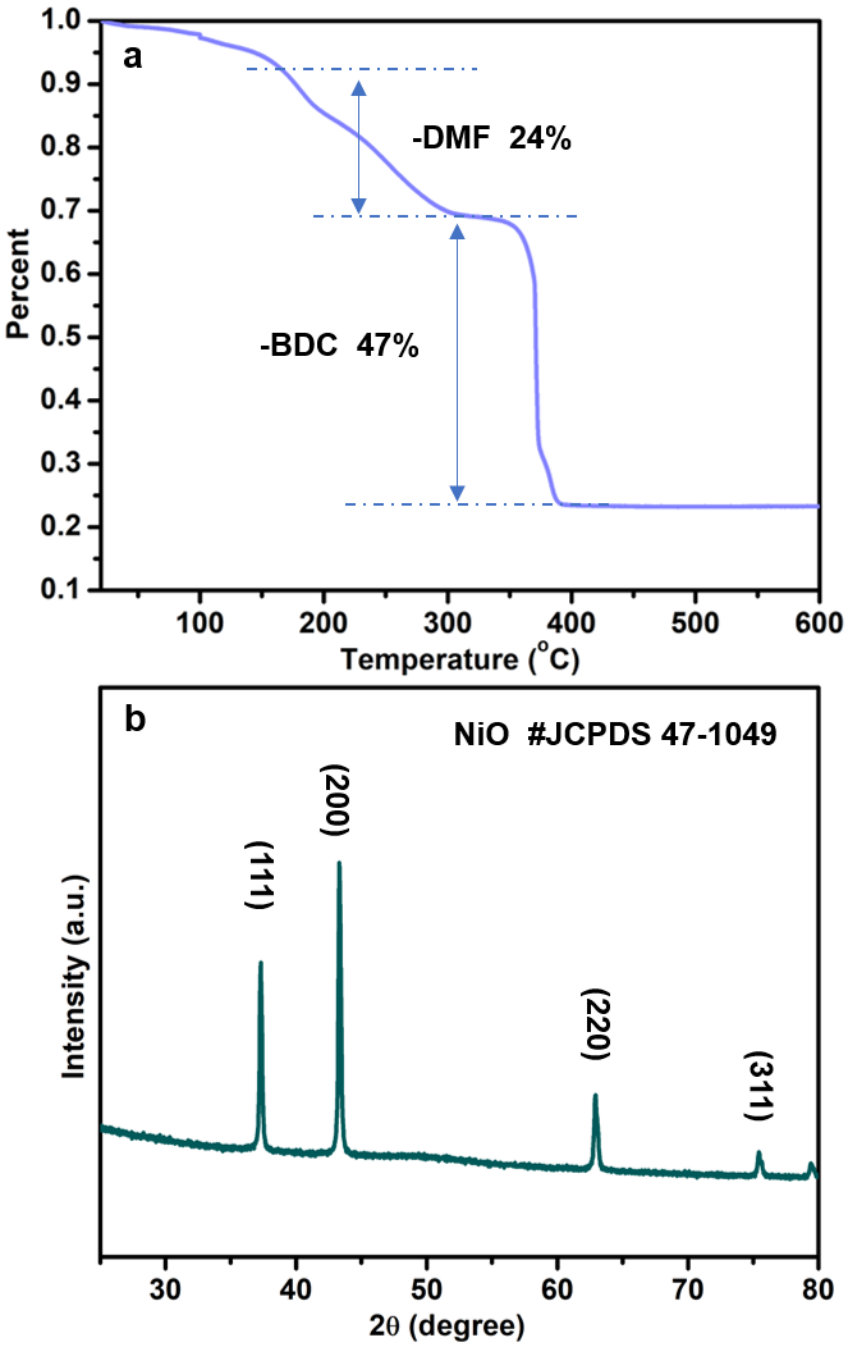

Figure S11. (a) TGA curve of the Ni-BDC sample under air atmosphere at a heating rate of 10 °C/min, and (b) XRD pattern of the residue from the TGA test of (a).

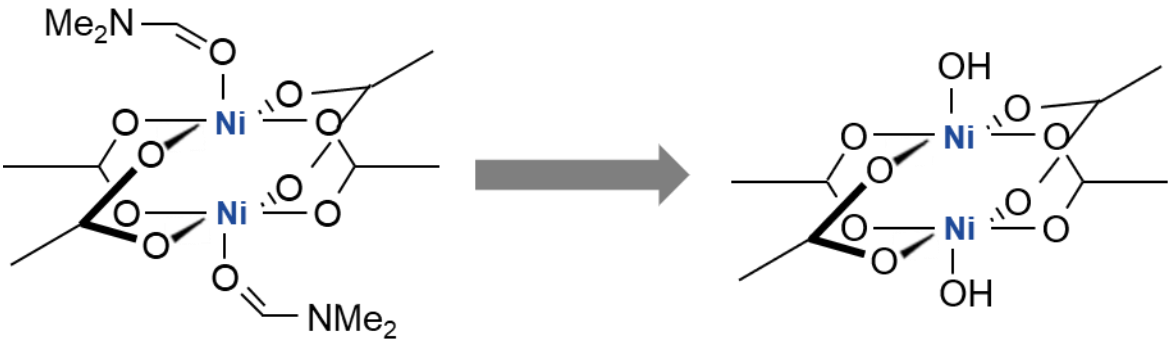

Figure S12. Illustration of replacement of solvent molecules (DMF) on each of the two Ni ions by hydroxo or aquo groups to complete the coordination of Ni ions.

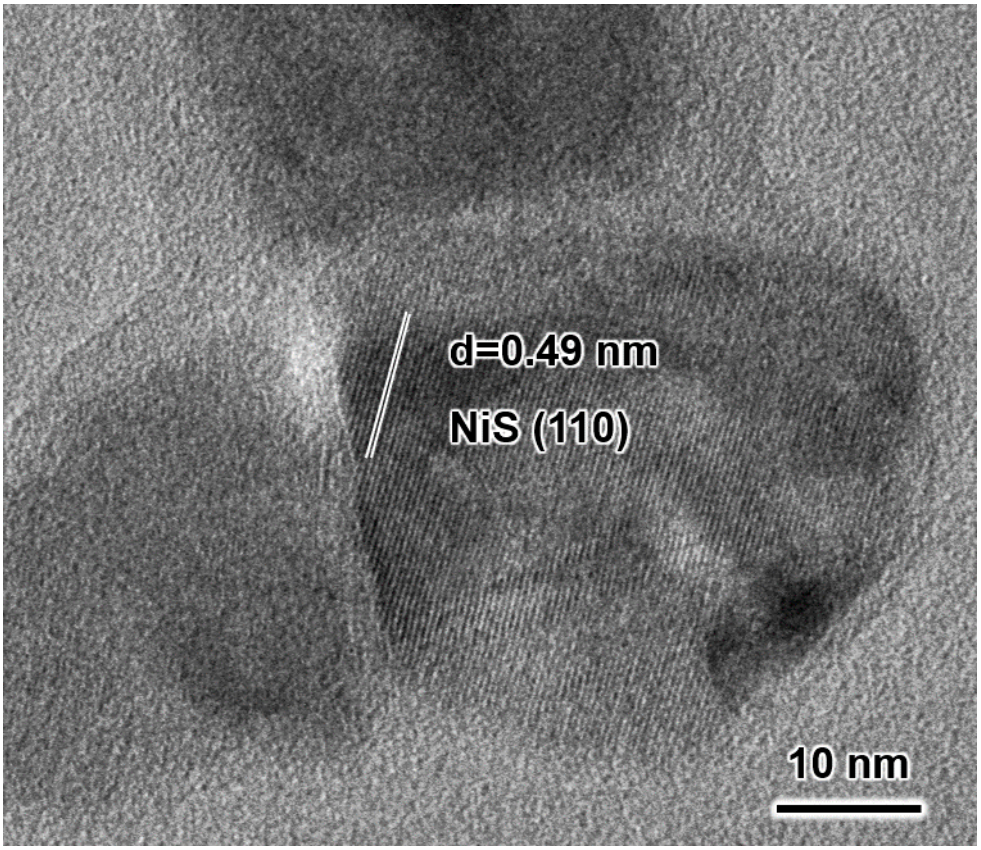

Figure S13. High-resolution TEM image of NiSO-BDC hollow nanoparticles. The interplanar spacing is 0.49 nm, which corresponds to d_{110} of NiS phase.

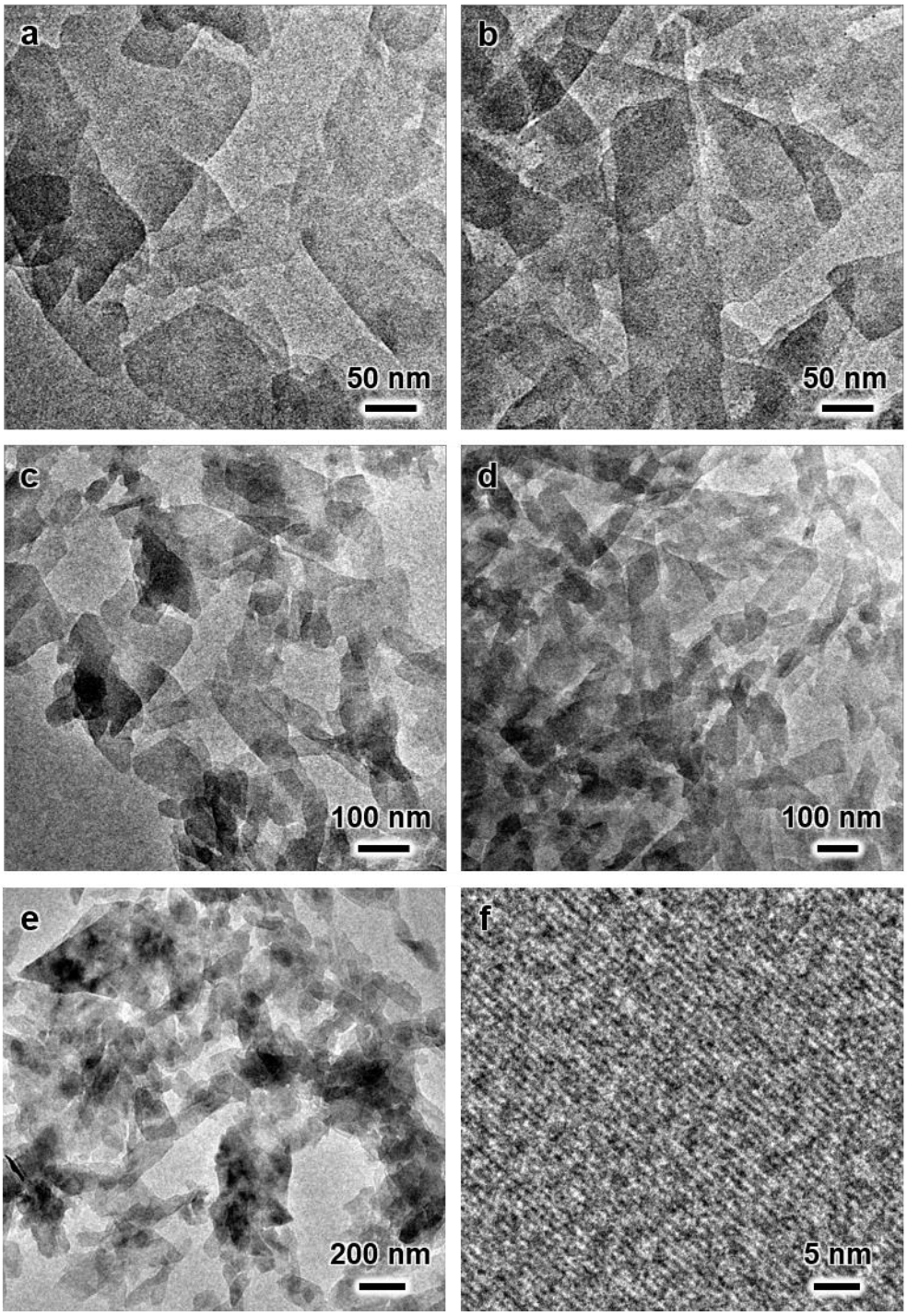

Figure S14. TEM images of the Ni-BDC sample after re-solvothermal treatment in a cosolvent (DMF: water: ethanol = 16:1:1).

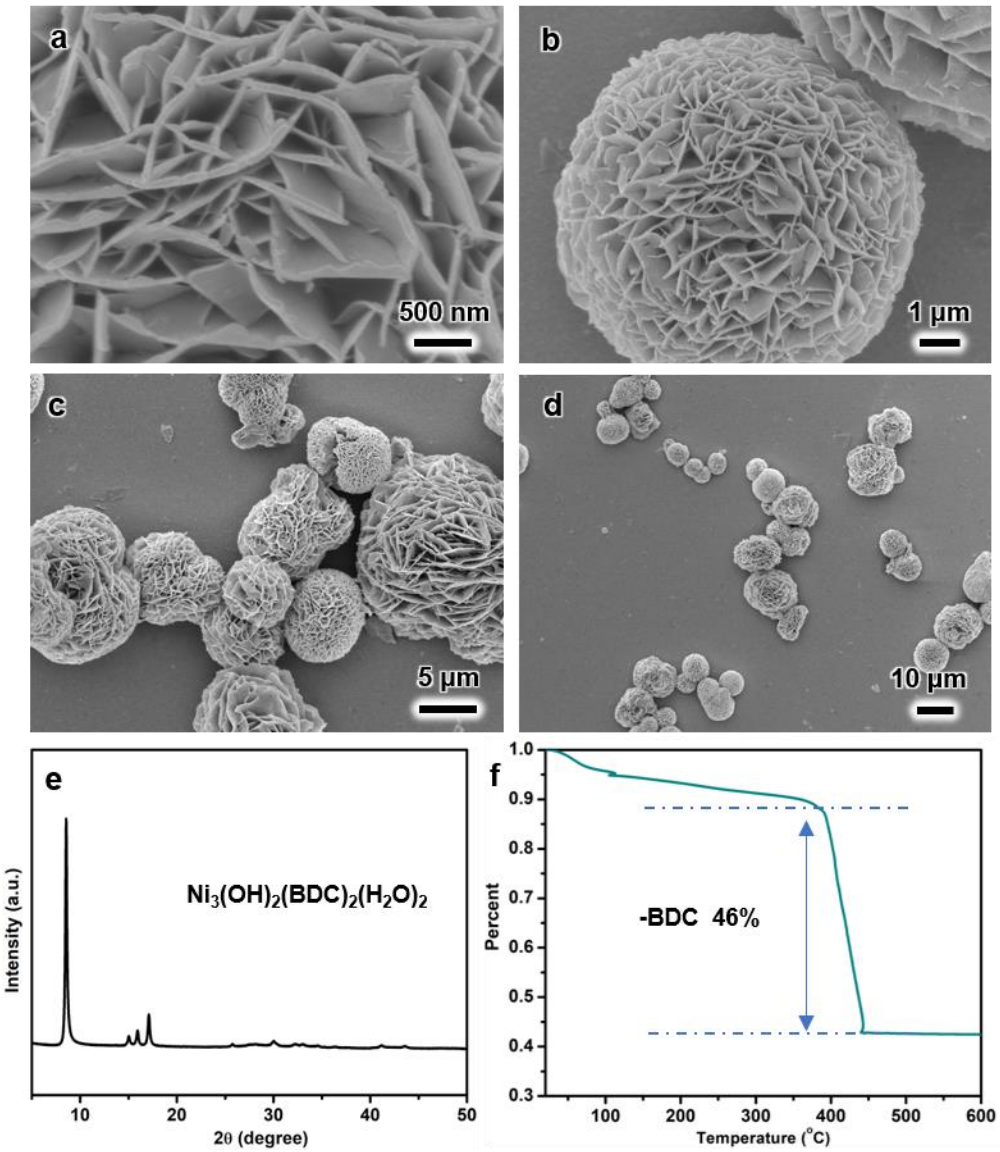

Figure S15. (a-d) SEM images, (e) XRD pattern, and (f) TGA curve of the as-prepared $Ni_3(OH)_2(BDC)_2(H_2O)_2$.

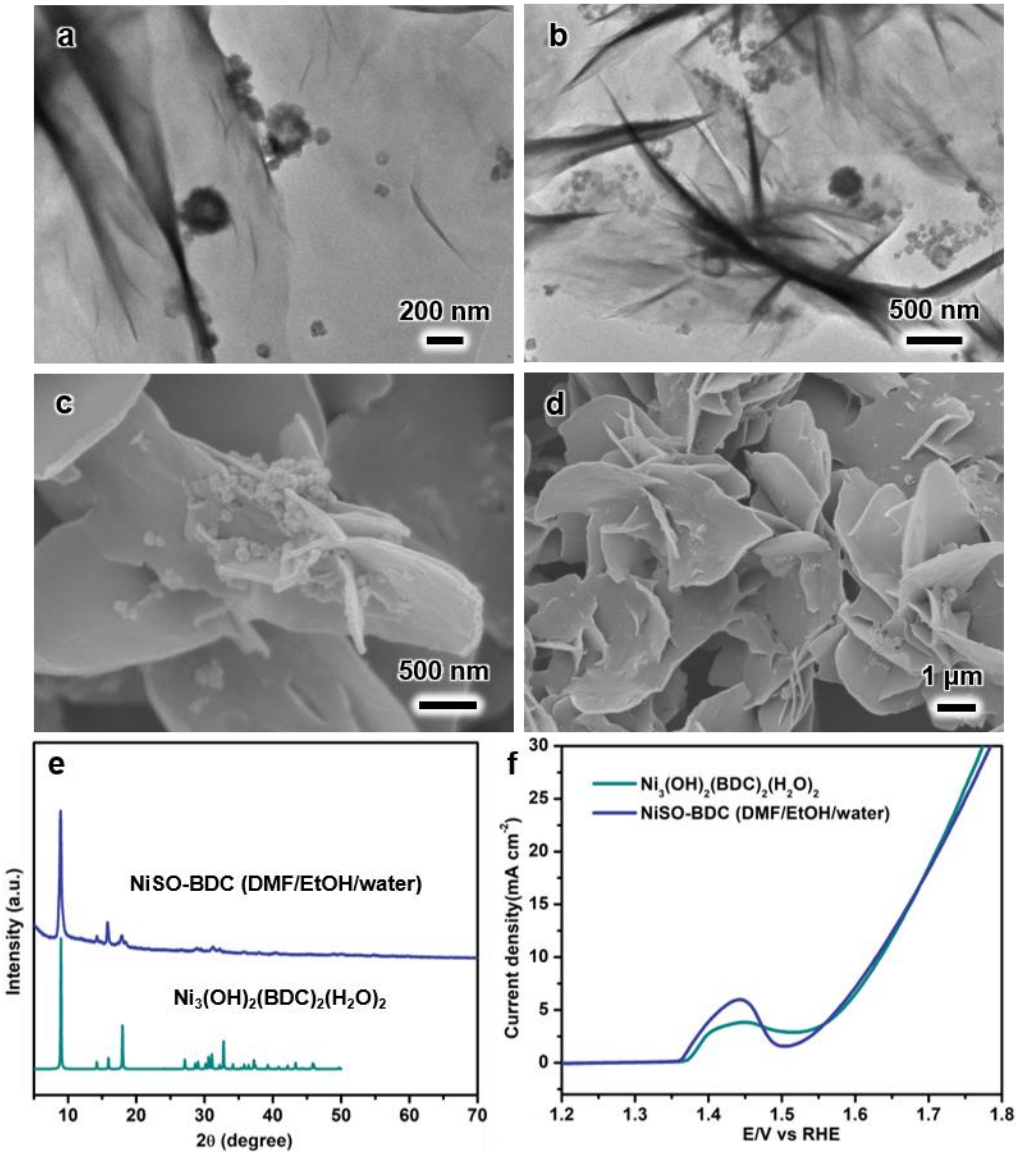

Figure S16. (a, b) TEM images, (c, d) SEM images of the as-prepared $Ni_3(OH)_2(BDC)_2(H_2O)_2$. (e) XRD pattern, and (f) OER tests of the as-prepared $Ni_3(OH)_2(BDC)_2(H_2O)_2$ and NiSO-BDC prepared directly using a cosolvent (DMF:ethanol:water = 16:1:1) at 120°C for 24 h.

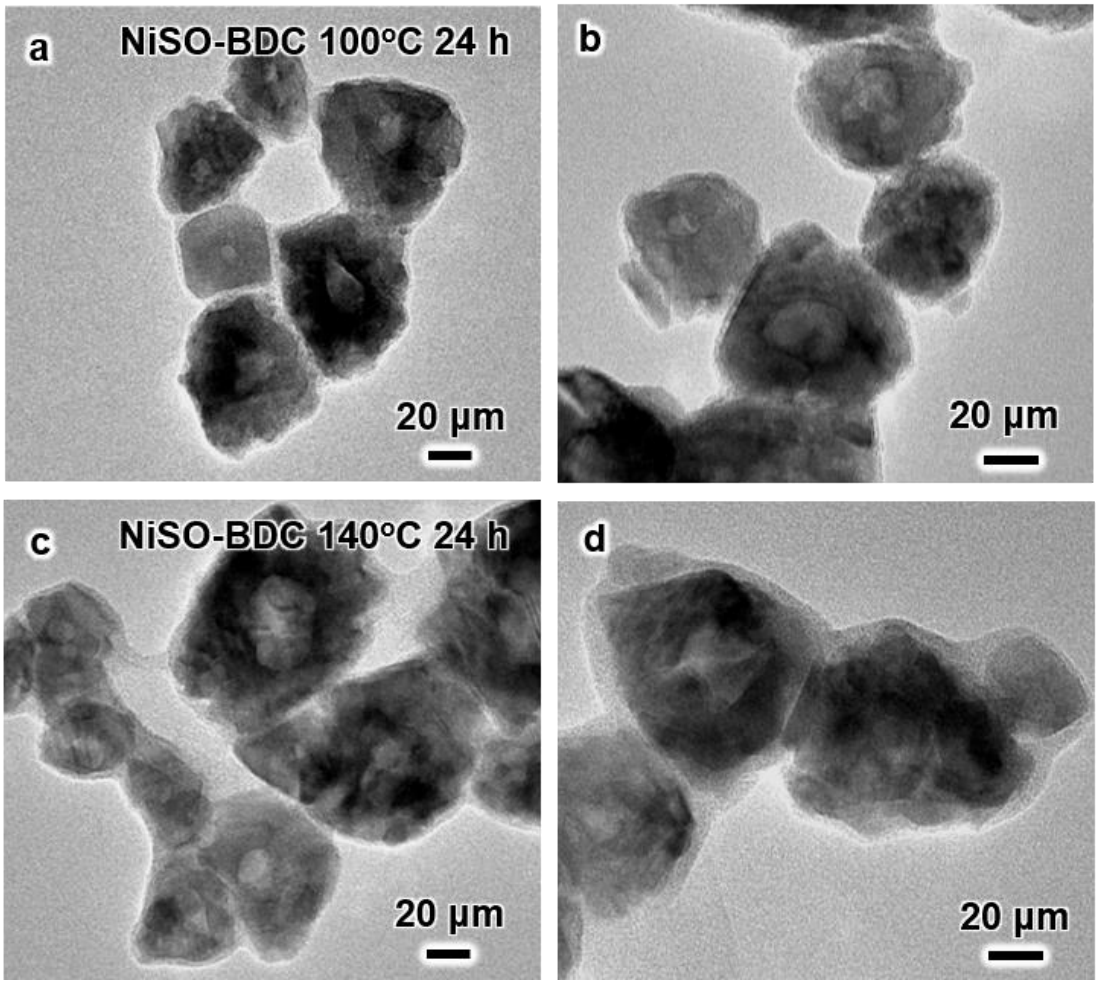

Figure S17. TEM images (a, b) and (c, d) are NiSO-BDC samples prepared at 100°C and 140°C for 24 h respectively.

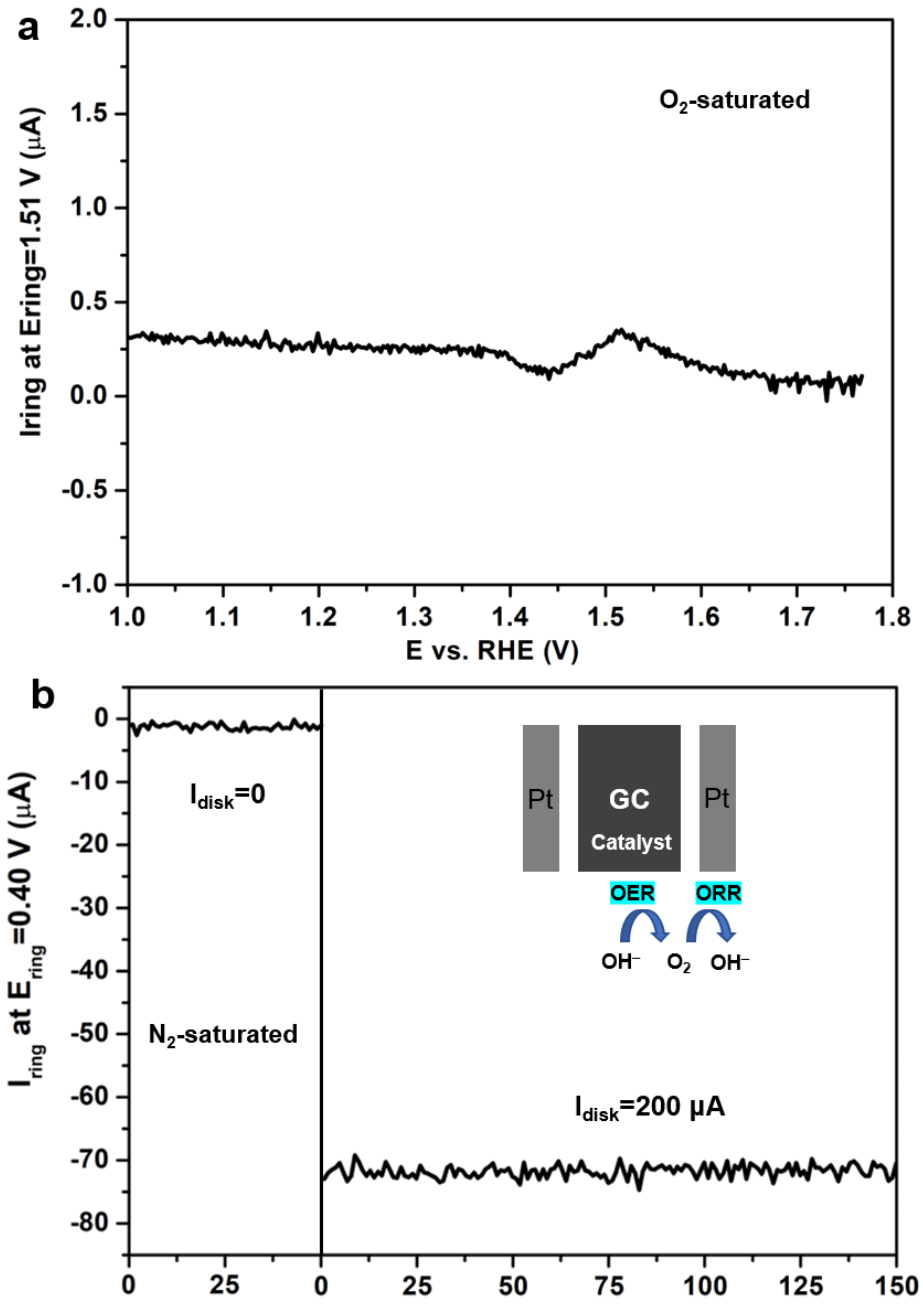

Figure S18. (a) The ring current of NiSO-BDC on a RRDE (1500 rpm) in O_2-saturated 0.1M KOH solution (ring potential: 1.51 V). (b) The ring current of NiSO-BDC on a RRDE (1500 rpm) in N_2-saturated 0.1M KOH solution (ring potential: 0.40 V).

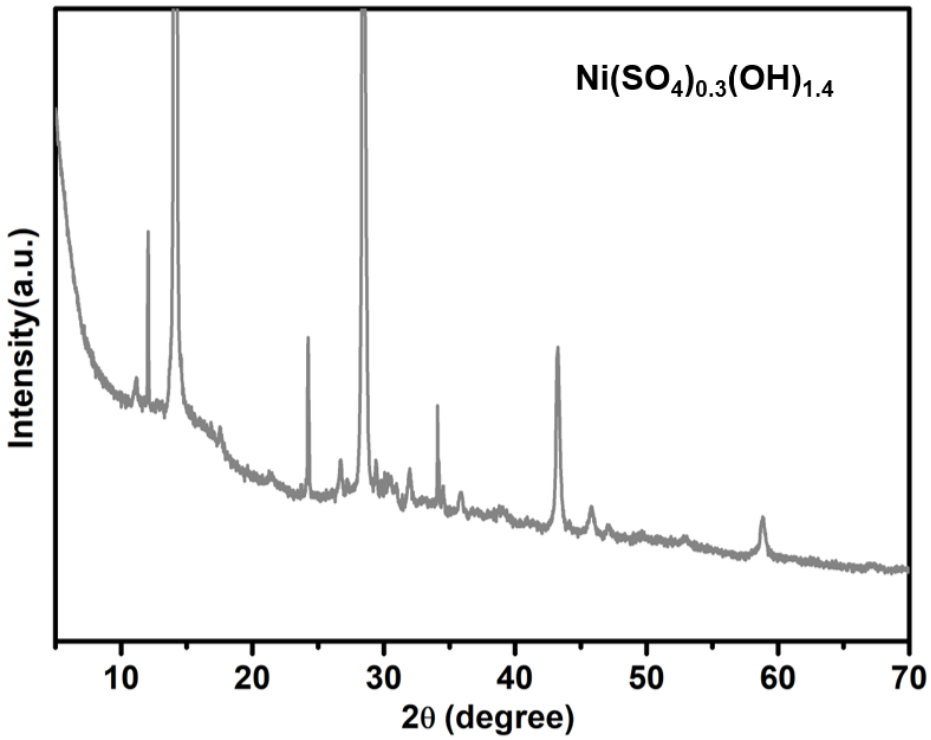

Figure S19. The XRD pattern of used NiSO-BDC sample. The phase can be mainly ascribed to $Ni(SO_4)_{0.3}(OH)_{1.4}$, which is consistent with the XPS spectra.

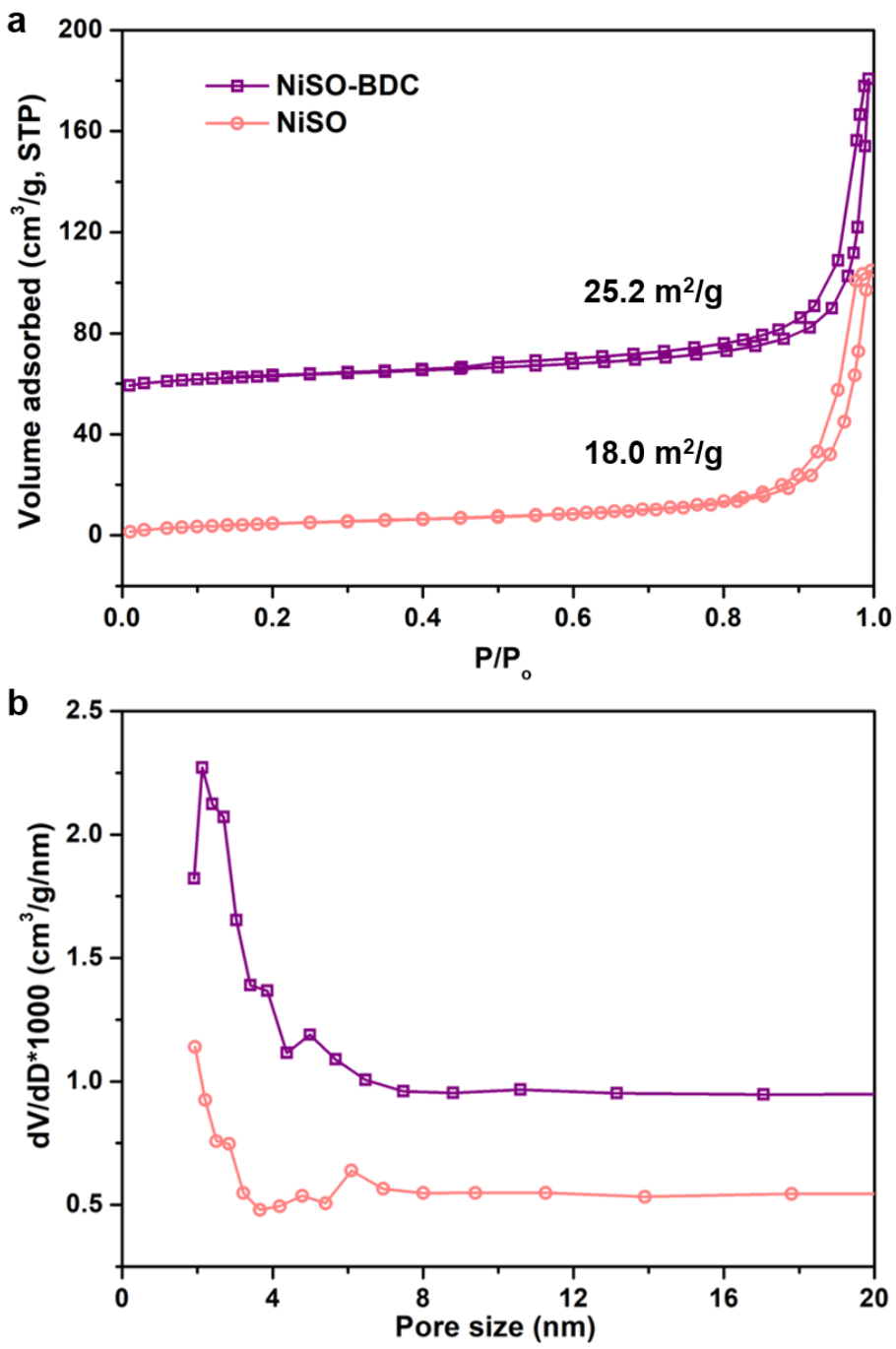

Figure S20. The N_2 adsorption−desorption isotherms and volumetric pore size distributions of NiSO and NiSO-BDC samples. The surface area of NiSO-BDC (25.2 m^2/g) is slightly increased compared to that of NiSO (18.0 m^2/g). Moreover, due to the porous structure of the MOF shell, the mesopores (~2.2 nm) of NiSO-BDC sample are increased.

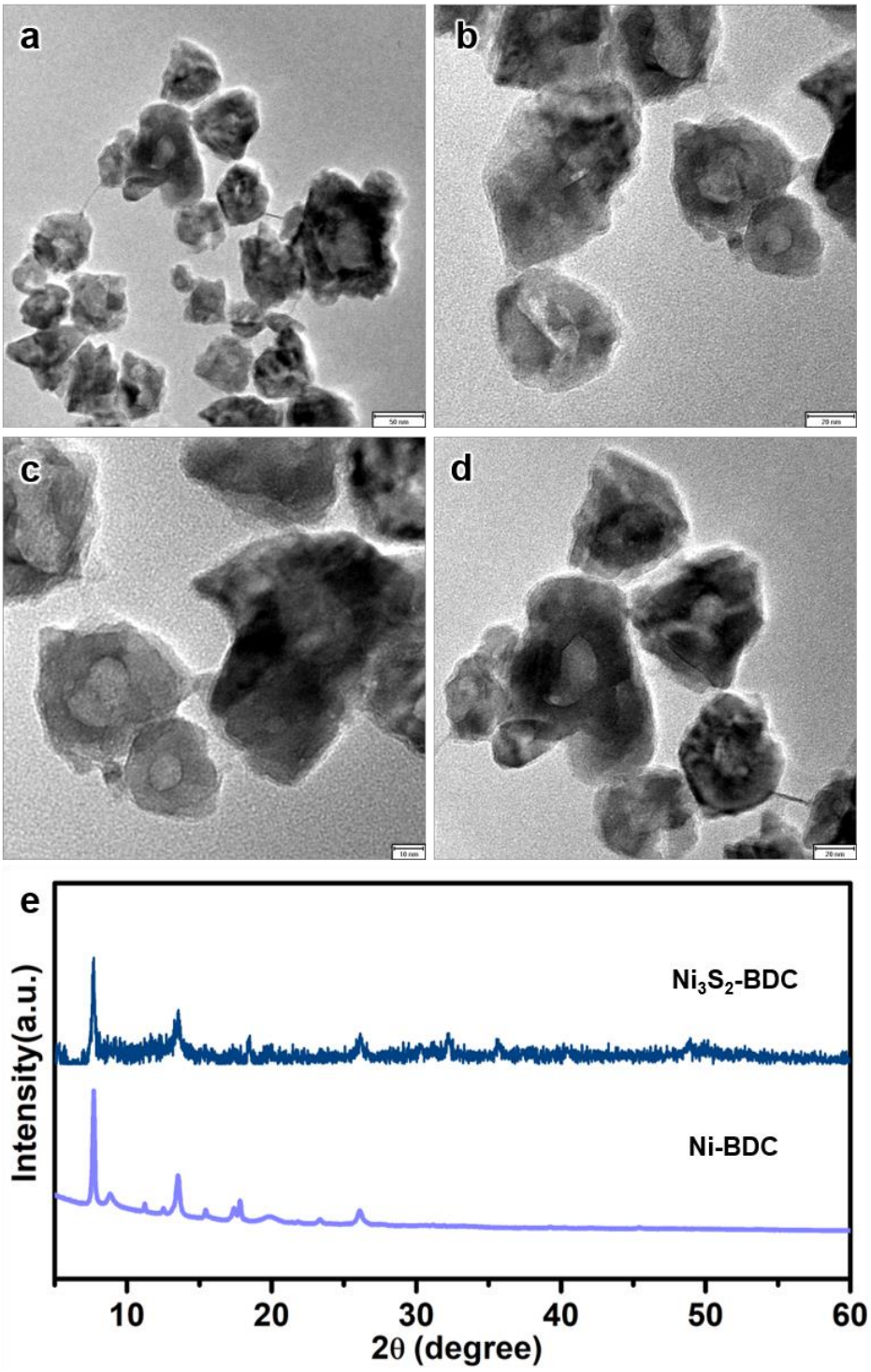

Figure S21. (a-d) TEM images of Ni_3S_2-BDC hollow nanoparticles, and (e) XRD patterns of Ni_3S_2-BDC and Ni-BDC. When Ni_3S_2 is directly used to react with H_2BDC, Ni-BDC shell cannot be formed uniformly due to the effect of organic groups adsorbed at the surface of Ni_3S_2.

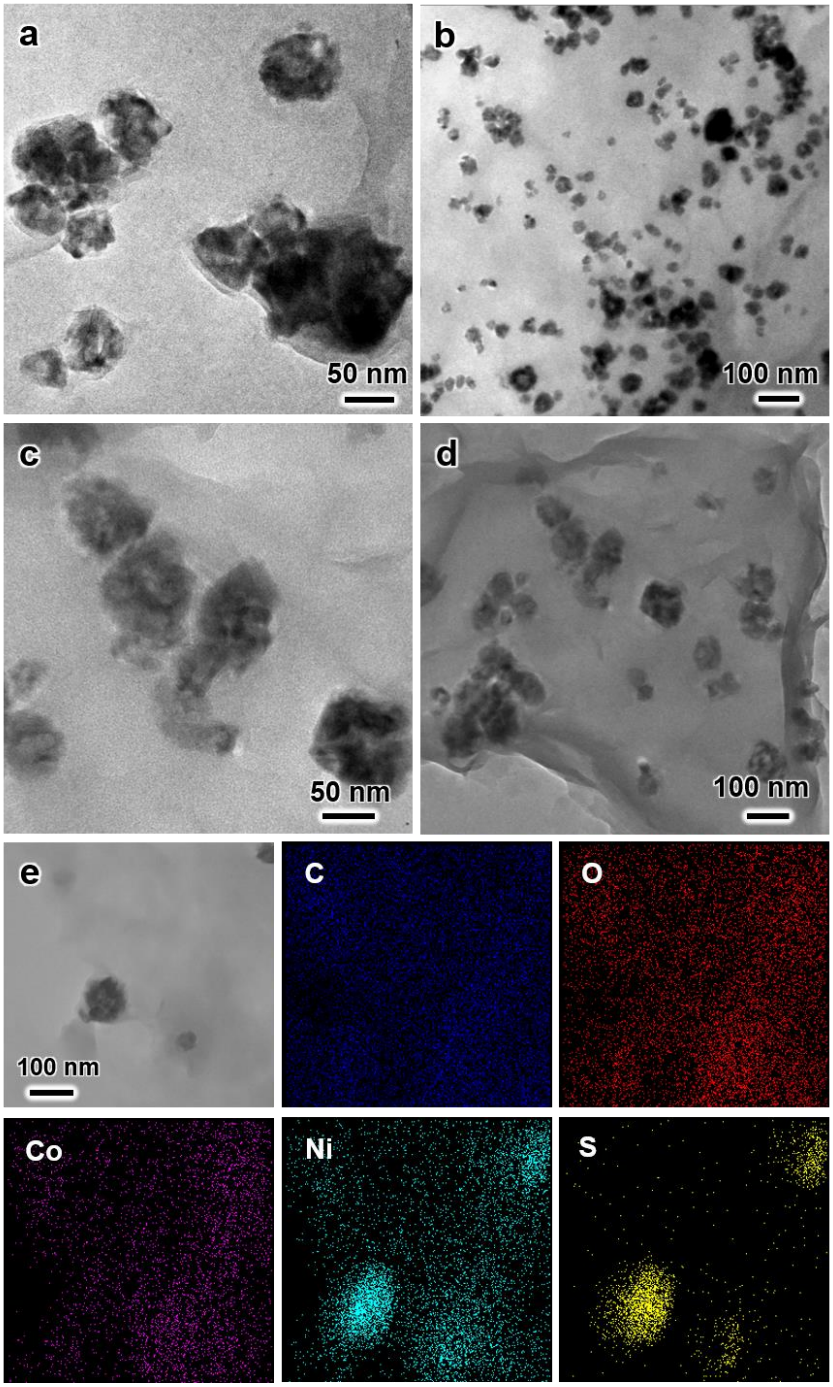

Figure S22. (a-d) TEM images and (e) element mapping images of NiSO hollow nanoparticles mixed with CoNi-BDC-TEA. This sample was prepared as follow: 30 mg of NiSO hollow nanoparticles was dispersed in 36 mL of a cosolvent of DMF, ethanol and DI water (DMF:ethanol:water = 16:1:1) by sonication for 20 min, and then 62 mg of terephthalic acid was added. Subsequently, 44 mg of $CoCl_2$ $6H_2O$ and 44 mg of $NiCl_2$ $6H_2O$ were added. After Co^{2+} and Ni^{2+} salts were dissolved, 0.4 mL of TEA was quickly injected into the above colloidal solution. Afterward, the colloidal solution was continuously stirred for 8 h at room temperature. Finally, the products were obtained via centrifugation, washed with ethanol for 3 times, and dried at 60°C.

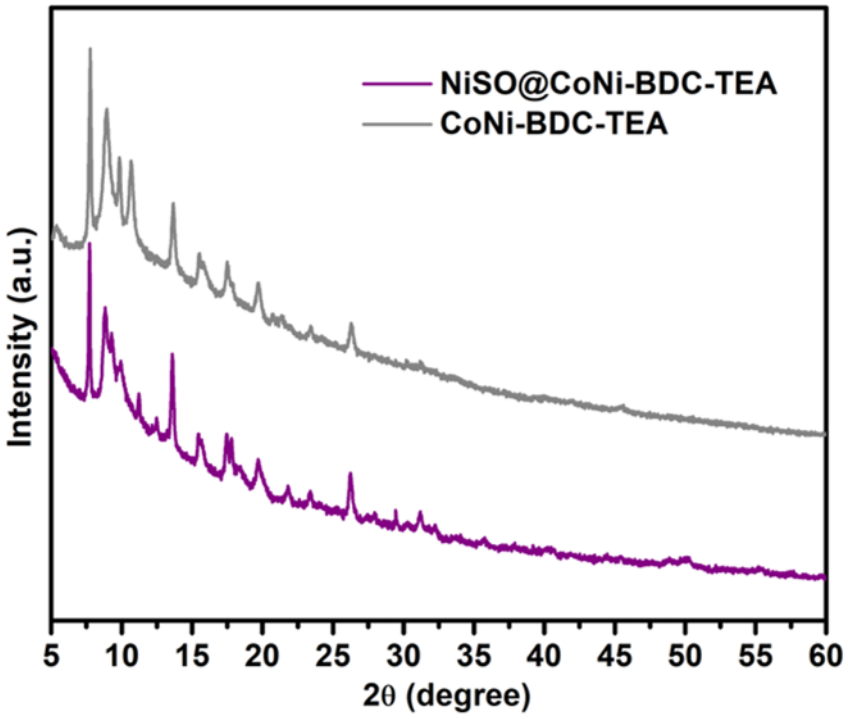

Figure S23. XRD patterns of CoNi-BDC-TEA and NiSO@CoNi-BDC-TEA.

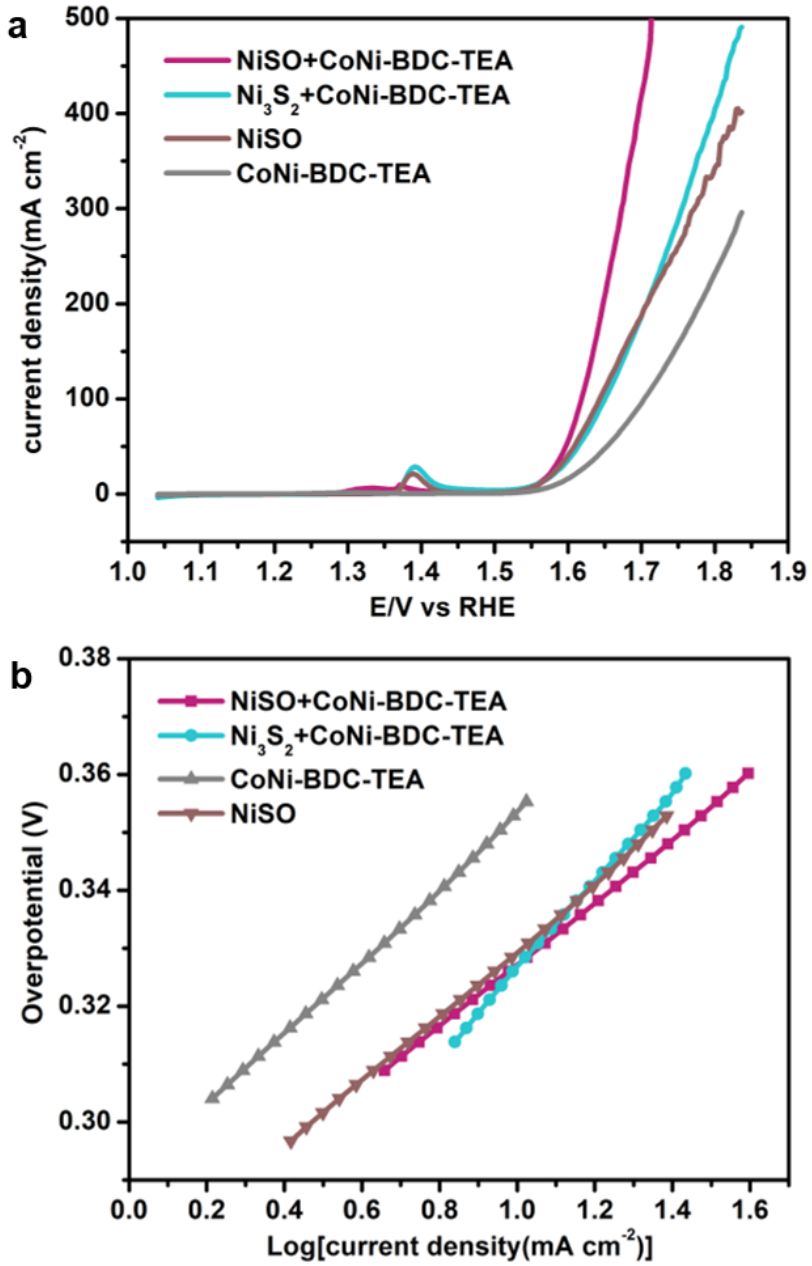

Figure S24. (a) LSVs and (b) the related Tafel plots of our prepared samples tested in 1.0 M KOH with addition of carbon.

Table S1. Carbon, hydrogen, nitrogen and sulfur (CHNS) analysis of the Ni-BDC sample.

Ni-BDC	C	H	N
wt%	41.93%	4.08%	4.68%

Table S2. The impedance parameters obtained by fitting

Electrocatalysts	Rs (Ω)	Rct (Ω)
NiSO	4.6	6.4
NiSO-BDC	3.2	5.0

Table S3. Comparison of the OER catalytic performance of our NiSO-BDC to other recently reported high-performance OER electrocatalysts using Ni_xS_y or MOFs**.**

Catalyst	**Electrolyte**	**Substrate**	η(mV)@10 mA·cm^{-2}	**Tafel slope** (mV·dec^{-1})	**Ref.** (year)
NiCo-UMOFNs	1.0 M KOH	GC	250	42	2016[2]
Fe/Ni/Co (Mn)-MIL-53	1.0 M KOH	GC	236@20 mA·cm^{-2}	52.2	2018[3]
[{$Fe_3(\mu_3$-O) $(bdc)_3\}_4$-{$Co_2(na)_4(L^T)_2\}_3$	pH = 13	GC	225		2017[4]
$Ti_3C_2T_x$–CoBDC	0.1 M KOH	GC	410	48.2	2017[5]
NiFe-MOF	0.1M KOH	NF	240	34	2017[6]
GO/Cu-MOF	0.5 M H_2SO_4	GC	119 (onset potential)	65	2013[7]
[$Co_2(\mu$-Cl)$_2$(bbta)]	1.0 M KOH	GC	292		2016[8]
PCN-224-Ni	pH = 7	FTO	450 (onset potential)	150	2016[9]
High-index faceted Ni_3S_2	1.0 M KOH	NF	260		2018[10]
N-Ni_3S_2	1.0 M KOH	NF	330@100 mA·cm^{-2}	70	2017[11]

MoS_2−Ni_3S_2	1.0 M KOH	NF	249	57	2017[12]
Ni-Fe-OH@Ni_3S_2	1.0 M KOH	NF	240@100 $mA \cdot cm^{-2}$	93	2017[13]
$Fe_{0.1}$-NiS_2 NA	1.0 M KOH	Ti	231@100 $mA \cdot cm^{-2}$	43	2016[14]

References

1. Wang, J. H.; Cheng, Z.; Bredas, J. L.; Liu, M., Electronic and Vibrational Properties of Nickel Sulfides from First Principles. *J. Chem. Phys.* **2007,** *127* , 214705-214713.

2. Zhao, S.; Wang, Y.; Dong, J.; He, C.T.; Yin, H.; An, P.; Zhao, K.; Zhang, X.; Gao, C.; Zhang, L.; Lv, J.; Wang, J.; Zhang, J.; Khattak, A. M.; Khan, N. A.; Wei, Z.; Zhang, J.; Liu, S.; Zhao, H.; Tang, Z., Ultrathin Metal–Organic Framework Nanosheets for Electrocatalytic Oxygen Evolution. *Nat. Energy* **2016,** *1*, 16184-16193.

3. Li, F. L.; Shao, Q.; Huang, X.; Lang, J. P., Nanoscale Trimetallic Metal-Organic Frameworks Enable Efficient Oxygen Evolution Electrocatalysis. *Angew. Chem., Int. Ed.* **2018,** *57*, 1888-1892.

4. Shen, J. Q.; Liao, P. Q.; Zhou, D. D.; He, C. T.; Wu, J. X.; Zhang, W. X.; Zhang, J. P.; Chen, X. M., Modular and Stepwise Synthesis of a Hybrid Metal-Organic Framework for Efficient Electrocatalytic Oxygen Evolution. *J. Am. Chem. Soc.* **2017,** *139*, 1778-1781.

5. Zhao, L.; Dong, B.; Li, S.; Zhou, L.; Lai, L.; Wang, Z.; Zhao, S.; Han, M.; Gao, K.; Lu, M.; Xie, X.; Chen, B.; Liu, Z.; Wang, X.; Zhang, H.; Li, H.; Liu, J.; Zhang, H.; Huang, X.; Huang, W., Interdiffusion Reaction-Assisted Hybridization of Two-Dimensional Metal-Organic Frameworks and $Ti_3C_2T_x$ Nanosheets for Electrocatalytic Oxygen Evolution. *ACS Nano* **2017,** *11*, 5800-5807.

6. Duan, J.; Chen, S.; Zhao, C., Ultrathin Metal-Organic Framework Array for Efficient Electrocatalytic Water Splitting. *Nat. Commun.* **2017,** *8*, 15341-15348.

7. Jahan, M.; Liu, Z.; Loh, K. P., A Graphene Oxide and Copper-Centered Metal Organic Framework Composite as a Tri-Functional Catalyst for HER, OER, and ORR. *Adv. Funct. Mater.* **2013,** *23*, 5363-5372.

8. Lu, X. F.; Liao, P. Q.; Wang, J. W.; Wu, J. X.; Chen, X. W.; He, C. T.; Zhang, J. P.; Li, G. R.; Chen, X. M., An Alkaline-Stable, Metal Hydroxide Mimicking Metal-Organic Framework for Efficient Electrocatalytic Oxygen Evolution. *J. Am. Chem. Soc.* **2016,** *138*, 8336-8339.

9. Usov, P. M.; Ahrenholtz, S. R.; Maza, W. A.; Stratakes, B.; Epley, C. C.; Kessinger, M. C.; Zhu, J.; Morris, A. J., Cooperative Electrochemical Water Oxidation by Zr Nodes and Ni–Porphyrin Linkers of a PCN-224 MOF Thin Film. *J. Mater. Chem. A* **2016,** *4*, 16818-16823.

10. Feng, L. L.; Yu, G.; Wu, Y.; Li, G. D.; Li, H.; Sun, Y.; Asefa, T.; Chen, W.; Zou, X., High-Index Faceted Ni_3S_2 Nanosheet Arrays as Highly Active and Ultrastable Electrocatalysts for Water Splitting. *J. Am. Chem. Soc.* **2015,** *137*, 14023-14026.

11. Chen, P.; Zhou, T.; Zhang, M.; Tong, Y.; Zhong, C.; Zhang, N.; Zhang, L.; Wu, C.; Xie, Y., 3D Nitrogen-Anion-Decorated Nickel Sulfides for Highly Efficient Overall Water Splitting. *Adv. Mater.* **2017,** *29*, 1584-1589.

12. Yang, Y.; Zhang, K.; Lin, H.; Li, X.; Chan, H. C.; Yang, L.; Gao, Q., MoS_2–Ni_3S_2 Heteronanorods as Efficient and Stable Bifunctional Electrocatalysts for Overall Water Splitting. *ACS Catal.* **2017,** *7*, 2357-2366.

13. Zou, X.; Liu, Y.; Li, G. D.; Wu, Y.; Liu, D. P.; Li, W.; Li, H. W.; Wang, D.; Zhang, Y.; Zou, X., Ultrafast Formation of Amorphous Bimetallic Hydroxide Films on 3D Conductive Sulfide Nanoarrays for Large-Current-Density Oxygen Evolution Electrocatalysis. *Adv. Mater.* **2017,** *29*, 404-410 .

14. Yang, N.; Tang, C.; Wang, K.; Du, G.; Asiri, A. M.; Sun, X., Iron-Doped Nickel Disulfide Nanoarray: A Highly Efficient and Stable Electrocatalyst for Water Splitting. *Nano Res.* **2016,** *9*, 3346-3354.